What's Inside The Box: Linear Fits of Unruly Impedances

Samuel English[1, *]

[1] *Department of Physics, University of California, Santa Cruz, CA 95064, USA*

(Dated: November 27, 2020)

Classical fundamentals of electromagnetism are well-defined: these pillars of thought and subsequent key equations allow us to easily probe unknown circuit configurations given a very limited set of experimental data recorded. We explore the determining of physical (and unphysical) parameters of these setups from a set of two-channel voltages, frequencies, an applied load resistance, as well as the phase offset between $V_{Ch.1}$ and $V_{Ch.2}$. We will analyze the impedance versus angular frequency of several mystery boxes (A,D,E) in order to determine these unknown circuit components. We find for mystery box A, C $\approx 8.14 * 10^{-8} \pm 1.77 * 10^{-16} F$ and suspect a single capacitor with some internal resistance; for mystery box D, R $\approx 9.83 \pm 0.257\Omega$ and C $\approx 5.55 * 10^{-7} \pm 4.4 * 10^{-9} F$, where we strongly support the model of a series RC circuit; last, we suggest that mystery box E, with L $\approx 0.00795 \pm 4.34 * 10^{-10} H$ and C $\approx 1.7 * 10^{-9} \pm 1.41 * 10^{-36} F$, contains a series LC configuration. More analysis with precise data and modeling must be conducted to cross-examine these results.

I. INTRODUCTION

Here, we intend to discover what components rest hidden within these mystery boxes through a statistical analysis of their parameters and theoretical relations, all to help reinforce the physical models we have for circuitry, and to build an integral understanding of the inner-workings of impedance, electronics, and working with uncertainty.

It is crucial to note the following: measurement error is not the main source of disagreement between the experiment's data and model, it comes from the approximate circuit model; all circuits have some inherent or stray inductance, capacitance, and resistance. We choose to leave some of these as negligible unless otherwise visible in full effect within the data. We perform multiple weighted linear regressions, utilizing propagation of error formulae to properly account for our deviation.

A. Thévenin's Theorem

Thévenin's theorem of linear circuit analysis helps us reduce the complexity of our circuit configuration. It states that any two-terminal network of resistors and voltage sources is equivalent to a single resistive component, R_0, in series with some voltage source, V_0 (think of a power supply or flashlight battery, Fig. 1).

When a load resistance, R_L, is connected to our power supply, a current, I, will then flow and the output voltage will be reduced to V, where

$$V = V_0 - IR_0 \tag{1}$$

We measuring the output voltage as a function of the load resistance; by graphing voltage versus the calculated current and assuming a linear fit, we may recover the slope and intercept, and therefore R_0 and V_0.

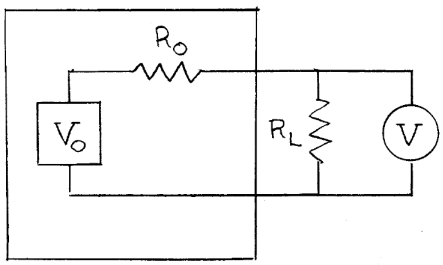

Figure 1. Thévenin's model for a power source. See Section II for preliminary experiment details [1].

B. Introduction to Impedances

Before examining our mystery boxes, it is crucial to review the theory behind complex impedance. The use of complex variables greatly simplifies our description of the relations between voltage and current, circuits containing reactances (inductors and capacitors). A reactance will take energy from the power source, store it in fields, either electric or magnetic, and return it to the circuit at a different time. This is in complete opposition to resistance, which will permanently dissipate the power absorbed into thermal energy.

Consider a simple resistor, R, through which a current, $I = I_0 \cos(\omega t)$, flows. The angular frequency, ω, is defined as $2\pi f$, where f is the recorded frequency in Hz. By Ohm's law, we see that the voltage across the resistor is then $V = RI = RI_0 \cos(\omega t)$. Thus, we conclude that the voltage, V, is in phase with our current, I.

However, if we now consider a pure inductance, for example, we see that this is not always the case. For some inductance, L, with a current $I = I_0 \cos(\omega t)$ going

* sdenglis@ucsc.edu

through it, the voltage across our component will be

$$V = L\frac{dI}{dt} = -\omega L I_0 \sin(\omega t) = \omega L I_0 \cos(\omega t + \frac{\pi}{2}) \quad (2)$$

Here, we state that the voltage leads the current by a phase offset of $\frac{\pi}{2}$, or 90°. Vice versa, the current lags the voltage by 90°.

The same procedure applies for capacitance, and we discover that a circuit with some pure capacitance, C, the voltage lags the current by phase angle of 90°:

$$V = \frac{Q}{C} = \frac{I_0}{\omega C}\sin(\omega t) = \frac{I_0}{\omega C}\cos(\omega t - \frac{\pi}{2}) \quad (3)$$

This, we were able to recover by setting our constant of integration to zero in the following:

$$Q = \int I dt = \int I_0 \cos(\omega t) dt = \frac{I_0}{\omega}\sin(\omega t), \quad (4)$$

While Ohm's law generally holds for the case of a simple resistor, having inductors and capacitors makes encapsulating our resistive term non-trivial.

We therefore construct a complex current $I_i = I_0 \sin(\omega t)$ in addition to the real current $I_r = I_0 \cos(\omega t)$, such that

$$I = I_0[\cos(\omega t) + i\sin(\omega t)] = I_0 e^{i\omega t}, \quad (5)$$

then allowing the following statement:

$$V = L\frac{dI}{dt} = (i\omega L)I_0 e^{i\omega t} = (i\omega L)I, \quad (6)$$

where V is now proportion to I by some complex impedance. We denote this constant of proportionality by Z, where in this case $Z = i\omega L$, the complex impedance for an inductor.

By a very similar procedure, we find that the complex impedance for a capacitor is represented by $Z = (\frac{1}{i\omega C})$.

These reactances can combine into a total impedance in different ways. For reactances in series, $Z = (Z_1 + Z_2 + ... + Z_N)$. Similarly, reactances in parallel add harmonically: $Z = (\frac{1}{Z_1} + \frac{1}{Z_2} + ... + \frac{1}{Z_N})^{-1}$

For each mystery box, we have either 1, 2, or 3 RLC (inductor-resistor-capacitor) components in series or in parallel. To determine the composition of each, we must compare the legitimacy of each linear model based on different combinations of RLC components.

C. Error Propagation

We are informed that the measurements in voltage have some inherent error on the order of $(0.03V_{obs})$. Furthermore, we choose to define the error in resistance as the following peace-wise function:

$$\sigma(R_\Omega) = \begin{cases} 0.1\Omega & \text{if } R < 100\Omega \\ 1.0\Omega & \text{if } R \geq 100\Omega \end{cases} \quad (7)$$

This allows for great simplification of our error in impedance. In plotting the the complex impedance as a function of the angular frequency, we must encapsulate some sigma term for our y-axis and error bounds. For our setup, we note that, thanks to our simplified Thévenin model, the current running through our mystery box systems, I, is equal to $\frac{V_2}{R}$, as well as $V_1 = I|Z|$, where V_1 and V_2 are the channel one and two voltages, respectively.

Using the general formula for error propagation, we find that for $|Z|^2 = R^2(\frac{V_1}{V_2})^2$ we obtain

$$\sigma_{Z^2}^2 = \left(\frac{\partial Z^2}{\partial V_1}\sigma_{V_1}\right)^2 + \left(\frac{\partial Z^2}{\partial V_2}\sigma_{V_2}\right)^2 + \left(\frac{\partial Z^2}{\partial R_S}\sigma_{R_S}\right)^2, \quad (8)$$

where R_S is representative of the sensing resistor which is applied in incremental steps to the mystery box and σ_{Z^2} is our error for the complex impedance squared. This equation then reduces quite nicely through algebraic manipulation and utilizing the definition of the impedance:

$$\sigma_{Z^2} = Z^2\sqrt{\left(0.0072 + \frac{4}{R^2}\right)} \quad (9)$$

The same procedure and algebra applies to obtaining an error for the admittance, $Y \equiv \frac{1}{Z}$ as σ_{Y^2}. Thus, using these methods, we can freely obtain standard deviation for our y-axis, and thus plot error bars for each linear relation found in our boxes.

We use the polyfit() module from numpy in Python for linear fits. This function returns the diagonal elements of σ^2 associated with each polynomial coefficient, yielding a standard deviation for the slope and intercept for each of our models. The weights are, by default, defined as $\frac{1}{\sigma}$. All chi-square tests carried out are reduced and take into account error as weighting, effectively amplifying our values due to the nature of our small uncertainties.

II. APPARATUS AND PROCEDURE

A. Preliminary Experiment

Before delving into the mystery boxes, we first explore the essence of the Thévenin model in detail. Given a simple circuit with some resistor, we wish to apply a load resistance R_L onto the circuit and find the output resistance R_0 as well as the open circuit voltage V_0. If we measure the output voltage and graph it as a function of the calculated current $I = \frac{V}{R}$, we may easily determine R_0 and V_0 through the slope and intercept, respectively:

$$V_0 = \text{y-intercept} \quad (10)$$

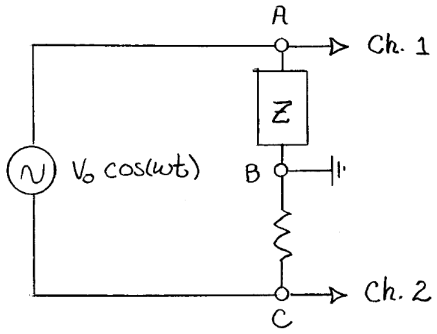

Figure 2. A circuit useful for analyzing the nature of Z, the complex impedance. This is the basic setup for all experiments carried out in the main laboratory experiment [1].

$$R_0 = \frac{V_0}{\text{x-intercept}} \tag{11}$$

B. Main Experiment: Mystery Boxes

One way to determine the contents of an unknown linear, two-terminal network is to pass a current $I = I_0 \cos(\omega t)$ through it and observe the voltage across the circuit while varying the generated frequency. Furthermore, it is helpful to first measure the DC impedance of the mystery box with an ohm-meter: inductors have small DC resistance, while capacitors have nearly infinite resistance.

To observe impedance as a function of frequency, we employ the circuit seen in Fig. 2. At each frequency, we purposefully choose an according sensing resistance so that the amplitudes of the two respective channel signals are comparable in magnitude.

An excellent method we use to analyze our data and see whether a straight-line fit can be made involves graphing several variations of functions of $|Z|$ and ω, from which component values can be recovered from the slope and intercept of our models.

For example: let's consider that we believe our circuit to be a parallel resonant circuit setup with the resulting equation, due to the observation of a resonant peak:

$$|Y|^2 = \frac{1}{R^2} + \left(\omega C - \frac{1}{\omega L}\right)^2 \tag{12}$$

We would then plot $|Y|^2$ vs. ω^2 for our high frequency points, where the slope would be C^2 and the intercept, $\frac{1}{R^2}$. As for our low frequency points, we would find that the plot for $|Y^2|$ vs. $\frac{1}{\omega^2}$ yields a slope of $\frac{1}{L^2}$ and an intercept of $\frac{1}{R^2}$. We further note that the resonant frequency, $\omega = \omega_0 = \frac{1}{\sqrt{LC}}$, allows for an independent check for any resonant circuit.

We are to examine a total of 3 boxes, as follows (where we decide to analyze those bolded):

- **Either** Box **A** or B
- **Either** Box C or **D**
- **Always** Box **E**

Each mystery box might be a single component (resistor, inductor, capacitor), two components in series or parallel, or a special type of resonant circuit (either all components in series, or the "realistic" kind with the resistor in series with the inductor, not all three components in parallel).

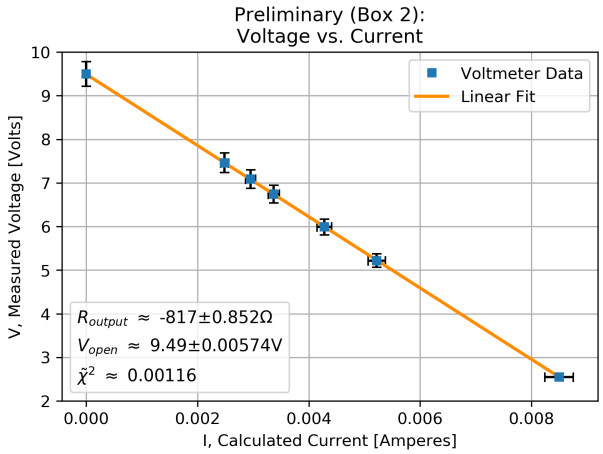

Figure 3. Measured circuit voltage versus calculated current flow using load resistance (R_L). We confirm Thévenin's theoretical model for an idealized power source via weighted linear regression on experimental data. Ohm's Law holds for linear circuity elements. (Reduced Chi-Square, $\tilde{\chi}^2$: 0.00116).

C. Secondary Experiment: Nonlinear Circuit Elements

Boxes J and K contain two-terminal nonlinear networks, where the magnitude of the response is not proportional to the magnitude of the stimulus. Hence, Ohm's law does not strictly hold as true: the current through such a device will not always be proportional to the voltage across it and thus the IV characteristic will not be a straight line.

Box J contains a silicon diode with a p-n junction. This device possesses an asymmetry which allows current to flow easily from the p-type to the n-type (forward direction), but with difficulty in the reverse direction. The simplest model for this junction is an analysis of the statistical physics of electrons inside of semiconductors, predicting that the current resulting when a voltage is applied to such a junction is:

$$I = I_S \left(e^{\frac{eV}{kT}} - 1\right) \tag{13}$$

The current current tends to increase with voltage for positive V, but will approach some reverse saturation current I_S whenever V is negative.

Box K contains a Zener diode, which behaves normally given V is greater than some negative voltage termed the Zener voltage. Otherwise, the diode begins to rapidly conduct, leading to a "Zener breakdown" effect.

III. RESULTS AND DISCUSSION

A. Preliminary Experiment: Output Impedance

We find the output (internal) resistance and open-circuit voltage of a source sub-circuit by: first, measuring its output voltage at five values of R_L (500 - 3000Ω); second, plotting the I-V curve (assuming linear fit); third, using the slope and intercept to recover these values.

Fig. 3 illustrates the linear nature of this circuit. We graph voltage versus current for the second preliminary box configuration with error bars included in both axes. Through a weighted linear fit we obtain an equation of the form $y = Ax + B$, with coefficients A, B equal to R_0, V_0 equal to $817 \pm 0.852\Omega, 9.49 \pm 0.00574V$, respectively. We can reliably state these values up to our significant figure cap, thanks to our model's reduced chi-square value, $\tilde{\chi}^2 = 0.00116$.

Thus, we reinforce the legitimacy of Kirchhoff's loop law as well as the applicability of Thévenin's model for a power source. We are able to reliably recover the open-circuit voltage and internal resistance for any mystery box which is model-able as such.

B. Main Experiment: Mystery Impedances

Box A: We first measure the DC resistance of each box to rule out some initial guesses. Box A's DC resistance reads OL (overload): thus, there must be a capacitor component hiding inside. We plot the various iterations of relations between impedance, admittance and angular frequency, eventually finding that our best linear relation stems from a resistor and capacitor in parallel. We fit our data to the following:

$$|Y|^2 \equiv \left(\frac{1}{R^2} + \left(\omega^2 C^2\right)\right) \tag{14}$$

This prediction cannot be completely justified because of the data taken, leading to an unruly chi-square value $\tilde{\chi}^2$: 6.15 (Fig. 7, 8). However, noticing how the intercept for our linear fit returns a resistance which is unphysical (negative), we could speculate that there is no resistive component whatsoever. Rather, we simply have a capacitor, some stray resistance, and bad data in the mix.

Further justification to this idea can be made with Fig. 4: we see strong support as to the existence of only a single element in the circuit, for a $\phi_{exp} \approx \pm\frac{\pi}{2}$. Subsequent chi-square test against observed and expected phase offsets reveal a strong correlation, $\tilde{\chi}^2$: 0.076.

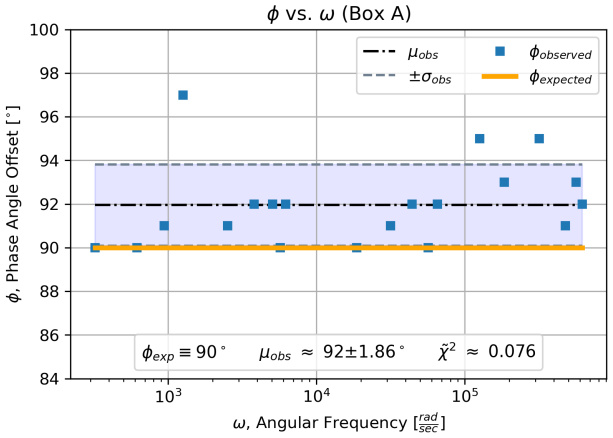

Figure 4. Box A's phase angle offset versus angular frequency for observed (blue) and expected (gold) values. We suspect the existence of only a single capacitor for box A (implying a constant phase offset of $\frac{\pi}{2}$). Chi-square test reveals that the phase offset strongly supports this theory. $\tilde{\chi}^2$: 0.076.

We carefully put forth the argument that mystery box A contains a single capacitor with some stray, internal resistance. Further testing would be needed as our current data has a potential outliar which skews the legitimacy of our linear fit.

Box D: Again, we measure the DC resistance and find that it reads OL. Thus, there must be at least a single capacitor in our setup. We find the best predictive model to arise from the assumption of a series RC (resistor and capacitor) circuit, in which the following equation holds:

$$|Z|^2 \equiv \left(R^2 + \frac{1}{(\omega C)^2}\right) \tag{15}$$

We recover values for R and C of $R \approx 9.83 \pm 0.257\Omega$ and $C \approx 5.55 * 10^{-7} \pm 4.4 * 10^{-9} F$ (Fig. 9, 10). Visually, the data fits quite nicely; furthermore, we obtain a reduced chi-square value $\tilde{\chi}^2$: 0.463.

While these results are modestly convincing, the phase offset plot (Fig. 5) is all the more so. We move forward in our assumption that a series RC model is accurate and create a set of expected phase angle offset values to compare our observed data against.

$$\phi_{exp} \equiv \tan^{-1}\left(-\frac{1}{\omega C R}\right) \tag{16}$$

Conducting yet another weighted, reduced chi-square test reveals the accuracy of our predictive phase offset model against the observed data values where $\tilde{\chi}^2$: 0.212.

We conclude that mystery box D contains a resistor and capacitor in series.

Box E: Here we come face-to-face with the problem child of our three mystery boxes. Initial DC resistance

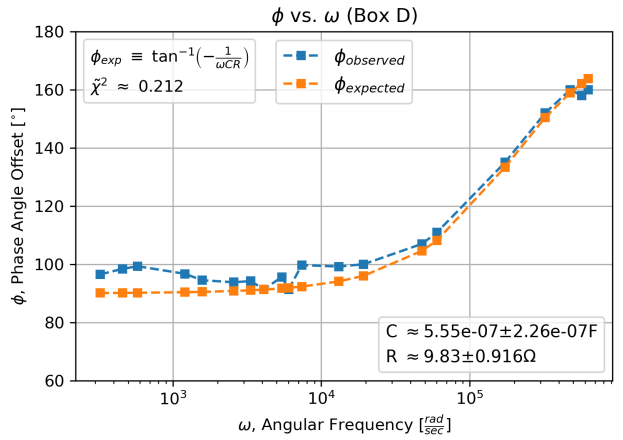

Figure 5. Box D's phase angle offset versus angular frequency (log) for observed (blue) and expected (gold) values. We suspect a capacitor and resistor in series with an expected phase offset $\phi_{exp} \equiv \tan^{-1}\left(-\frac{1}{\omega CR}\right)$. Using values for C and R recovered from our slope and intercept in Fig. 9, we find that our subsequently calculated ϕ_{exp} strongly fits ϕ_{obs}. $\tilde{\chi}^2$: 0.212.

readings taken indicate the presence of a capacitor (OL). Immediately, after plotting the admittance^2 versus the angular frequency^2, we observe a resonant peak centered around $\omega_0 = 2.64 * 10^5[\frac{rad}{sec}]$ (Fig. 11).

Now, we narrow down the possibilities to a couple of cases: either we have a series RLC circuit, a realistic parallel RLC setup in which the resistor is in series with the inductor (but not the capacitor), or simply a resonant LC (inductor and capacitor) circuit with negligible resistance. Must be in series due to DC resistance OL reading.

On the front of the first two cases, calculations and plots were non-trivial. First, we assumed the realistic case, where values quickly began to fall apart and chi-square values were unnecessarily large. So, we instead fall back to the series RLC setup, with an impedance equation:

$$|Z|^2 \equiv R^2 + \left(\omega L - \frac{1}{(\omega C)^2}\right) \tag{17}$$

Because resonant circuits have both ω and $\frac{1}{\omega}$ dependence, we plot both the high and low frequency values, well away from resonance, where both effects play large, separate roles as straight lines. We carefully select regions of the graph where each effect is prominent, and create linear fits from the data within that regime.

For our lower frequencies we plot impedance^2 versus angular frequency^2 and recover a capacitance of C $\approx 1.7 * 10^{-9} \pm 1.41 * 10^{-36} F$, with quite some confidence, as our reduced chi-square value $\tilde{\chi}^2$: 0.304 (Fig. 12).

For higher frequencies, the inductance should dominate, where we then plot impedance^2 versus inverse angular frequency^2. Again, we carefully select points away from resonance for which we can reliably extract a value of L $\approx 0.00795 \pm 4.34 * 10^{-10} H$, with a reduced chi-square statistic $\tilde{\chi}^2$: 0.732 (Fig. 13).

For both graphs pertaining to mystery box E, we find that the intercept provides no meaningful interpretation. It seems to vary in actual value and (because of its negative sign) returns NaN when actually computing the resistance. So, we became puzzled as to the true nature of this box, but found some reassurance in checking against the predicted resonant peak location as well as the phase angle offset (resonant frequency is a probe of L and C):

$$\omega_0 = \frac{1}{\sqrt{LC}} \tag{18}$$

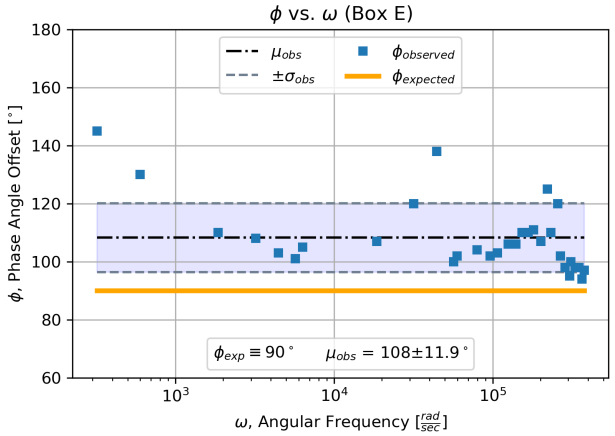

Figure 6. Box E's phase angle offset versus angular frequency (log) for observed (blue) and expected (gold) values. Multiple attempts to fit the experimental data to different RLC-circuit phase offset formulae proved to be unfruitful. Here, we show the largely inaccurate nature of the data taken. No apparent pattern emerges: thus, we argue that this may be a sign of either (1) bad data (2) a systematic source of error or (3) an incomplete model. No real conclusions can be drawn.

We, using predicted values from our model, expect the resonant peak to appear at roughly $\omega_{0_{exp}} \approx 2.72 * 10^5[\frac{rad}{sec}]$, whereas the observed peak occurs at $\omega_{0_{obs}} \approx 2.64 * 10^5[\frac{rad}{sec}]$ (Fig. 11). Considering the complete lack of extra data surrounding the resonant peak as well as whatever other error encompasses the observed data values, these match surprisingly well.

Now, we tentatively argue that mystery box E contains a series LC circuit with some inherent resistive components which skew the data. Being a bit confused with our findings from graphing impedance relations, we look to phase plots to provide us some hopeful guidance.

If our configuration were to be a series LC circuit, we would expect a phase offset $\phi_{exp} \approx \pm\frac{\pi}{2}$. Looking at Fig. 6, we do not directly observe this relation. However, we argue that due to the poor set of data provided, further testing would be needed in order to definitively conclude what rests inside of mystery box E. We attempted plot-

ting other relations for ϕ_{exp}. Here is the equation for our RLC series setup where some conversion is necessary to output in degrees, for example:

$$\phi_{exp} = \tan^{-1}\left(\frac{\omega L - \left(\frac{1}{\omega C}\right)}{R}\right) \tag{19}$$

While this may seem helpful, all formulas required some value for R, which we could not seem to pinpoint with any degree of accuracy. After some degree of messing around, we happened upon a natural-looking fit for an RLC series model; however, all of the parameter choices were extremely arbitrary and had no physical bearing or significance to our mystery box.

This discrepancy could potentially be justified by (1) bad data and or (2) a systematic source of error for this box. Fig. 6 illustrates the expected outcome for a series LC circuit, while the observed values seem (1) scattered with no pattern, indicative of poor values and (2) consistently shifted above ϕ_{exp} by $\Delta\phi \approx 18°$, a sign of systematic error.

Considering all the aforementioned points, we carefully argue that a series LC configuration with stray resistance could predict the observed values in box E's experiment; however, due to a lack of proper data, our analysis cannot prove anything at or above a significant standard.

C. Nonlinear Circuit Elements

We depict and observe the nature of our ordinary silicon diode within box J: in accordance with Eq. (13), we notice the current spikes quite sharply at some critical voltage amount (Fig. 14). This curve of exponential nature at voltages strictly above zero aligns with what we expected.

Similarly, box K, containing a Zener diode, experiences an exponential increase in current for positive voltage values; however, as we increase the voltage negatively, we approach a critically steep drop-off into a reverse-bias state. We note that the Zener diode in box K behaves like an ordinary diode given a voltage greater than our critical Zener voltage. When below this threshold, the diode begins to rapidly conduct again (Fig. 15).

Both of these diode processes can be modeled through a linear fitting of the logarithm of the current against the voltage for $V \approx +100mV$ and greater, where the "1" can thereby be neglected in our equation.

IV. CONCLUSIONS

Our preliminary experiment helped to reinforce the legitimacy and practicality of Kirchhoff's loop law as well as the applicability of Thevenin's model for a simplified power source. We were able to reliably recover the open-circuit voltage and internal resistance values for a given box full of electrical components. Amazingly, this concept was transferable to our mystery box setup, which allowed for a reduction in complexity when analyzing each configuration. Upon fully exploring each mystery box's potential, we put forth the following hypotheses:

- **Box A:** contains a **single capacitor** with **negligible resistance.**
- **Box D:** contains a **series RC** , with a small resistive component.
- **Box E:** contains a **series LC** configuration with **stray resistance.**

We carefully hypothesize that mystery box A contains a single capacitor component with some stray, internal resistance. Further testing would be needed as our current data has a potential outliar, causing a massive skewing to our weighted fit and subsequent chi-square analysis.

We are almost certain of mystery box D's composition as a series RC circuit given the accuracy and legitimacy of our goodness of fit test values.

Considering all of the aforementioned points raised, we speculate the existence of a series LC configuration with stray resistance in mystery box E. This could accurately predict the observed values in box E's impedance plots; however, due to a lack of proper data, our analysis cannot prove anything at or above a significant standard or explain the massive discrepancy in phase offset plot.

We leave hoping to have given some crucial insight as to the inner workings behind the statistics, graphing, error, and analysis for this type of project: in future work, we suggest for others to retake data as diligently as possible and cross-examine the results found here for the same mystery boxes.

Furthermore, all of our models are simplified and approximate: to fully encapsulate the minutiae of our observed values, broader, more encapsulating models are necessary.

ACKNOWLEDGMENTS

SE is a part of the PHYS 133, Intermediate Laboratory course. None of this information is presented for journal publication, only for writing improvement.

BIBLIOGRAPHY

[1] George Brown. *Laboratory Manual: Physics 133*. University of California, Santa Cruz, Spring 2020.

APPENDIX

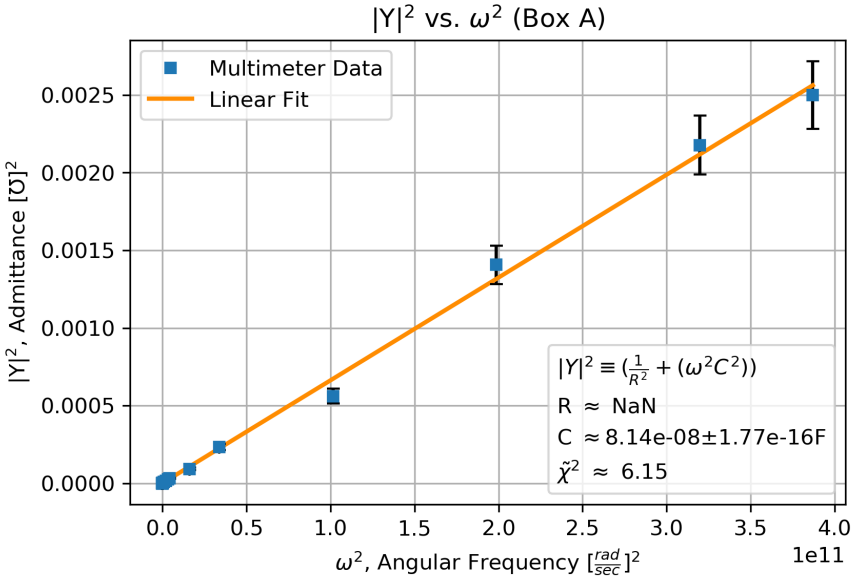

Figure 7. Mystery box A's admittance^2 versus angular frequency^2 in linear space. Here, we conduct a weighted linear fit for $|Y|^2 \equiv \left(\frac{1}{R^2} + \left(\omega^2 C^2\right)\right)$ assuming the circuit consists of a resistor and capacitor in parallel. We find that the intercept is unphysical (extremely small and negative), and our capacitance $C \approx 8.14 * 10^{-8} \pm 1.77 * 10^{-16} F$. Although this parallel RC model represents the best out of all possible linear models explored, no clear-cut conclusions can be made with our modest chi-square value $\tilde{\chi}^2$: 6.15.

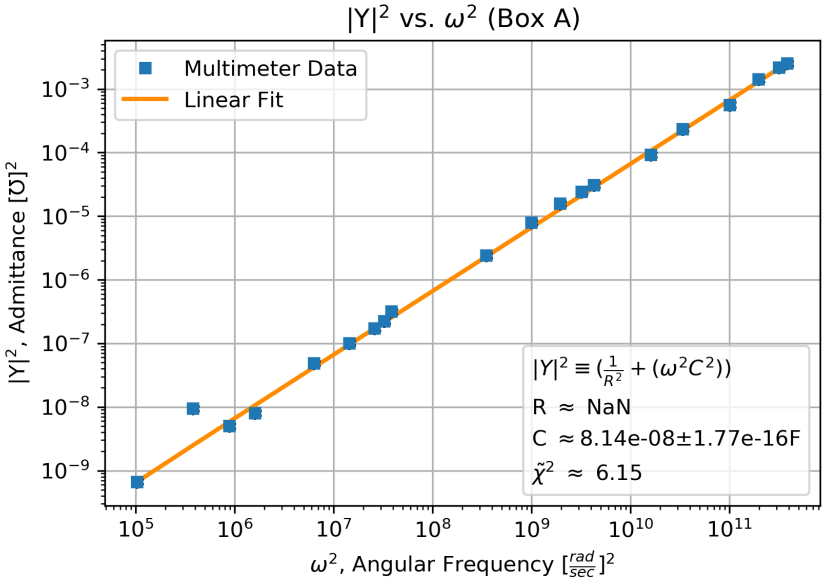

Figure 8. Mystery box A's admittance^2 versus angular frequency^2 in logarithmic space. The log plot helps illustrate the discrepancies in our data: if not for the single, lower frequency data point, our model would have been much more precise in predicting values. Again, no solid conclusions can be drawn: further data taking would be expected.

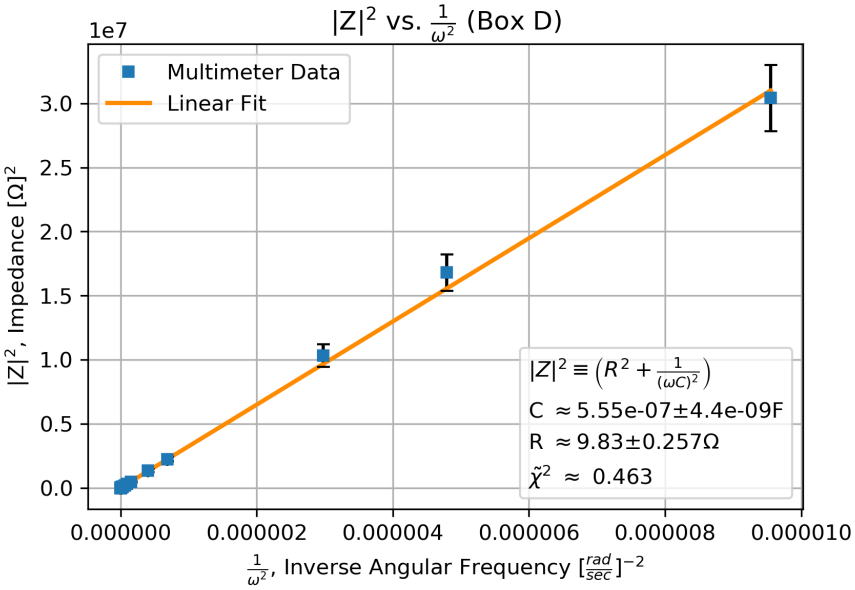

Figure 9. Mystery box D's impedance^2 versus inverse angular frequency^2 in linear space. Here, we conduct a weighted linear fit for $|Z|^2 \equiv \left(R^2 + \frac{1}{(\omega C)^2}\right)$ assuming the circuit consists of a resistor and capacitor in series. We extract values for C and R of C $\approx 5.55 * 10^{-7} \pm 4.4 * 10^{-9} F$ and R $\approx 9.83 \pm 0.257\Omega$. This series RC model serves as the best possible fit, with a reduced chi-square value $\tilde{\chi}^2$: 0.463.

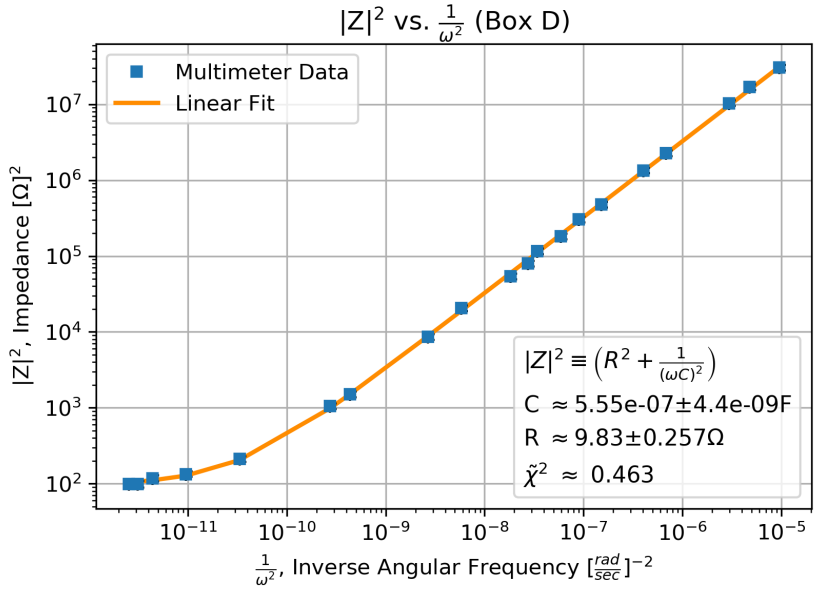

Figure 10. Mystery box D's impedance^2 versus inverse angular frequency^2 in logarithmic space. The log plot helps illustrate the spread of observed data points taken on the global scale of angular frequencies, further reinforcing the visual accuracy of our linear fit.

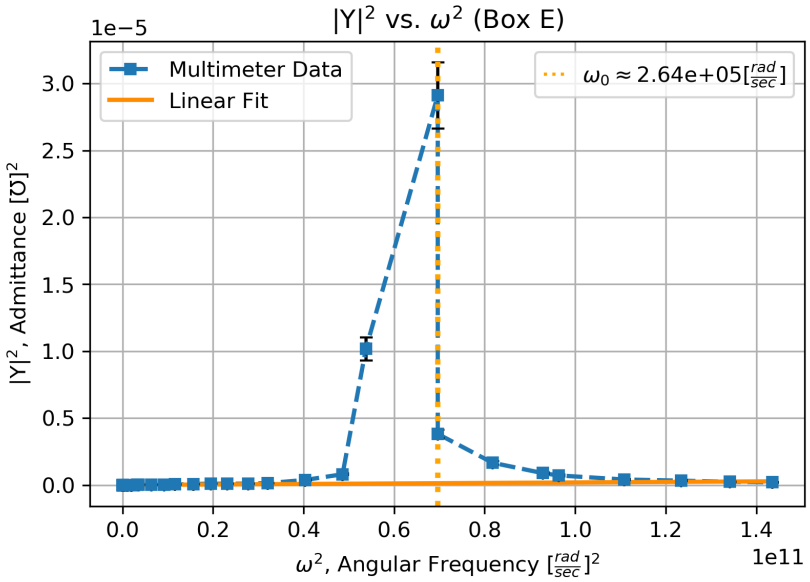

Figure 11. Mystery box E's admittance^2 versus angular frequency^2 in linear space. Here, we can easily observe the resonant nature of the unknown circuit configuration, as well as pinpoint the value of ω at the peak of resonance, $\omega_0 \approx 2.64 * 10^5[\frac{rad}{sec}]$. No simple linear fit will suffice. Instead, further plotting in different variable space for high and low frequencies is necessary.

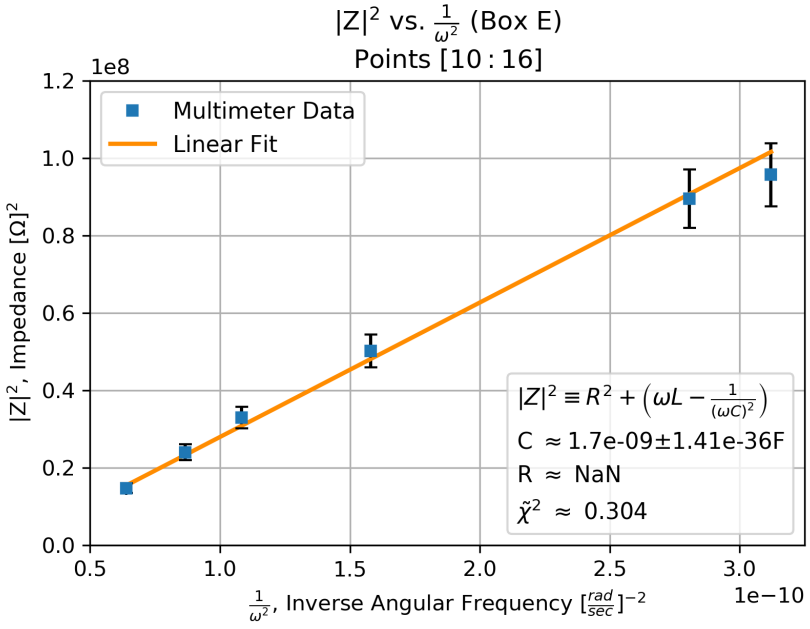

Figure 12. Mystery Box E's impedance^2 versus inverse angular frequency^2. We purposefully truncate data, hoping to isolate high frequency values for our weighted linear regression (points [10:16] from supplied data table). Utilizing the assumption of a series RLC circuit and the subsequent equation $|Z|^2 \equiv R^2 + \left(\omega L - \frac{1}{(\omega C)^2}\right)$, we calculate the value of C $\approx 1.7 * 10^{-9} \pm 1.41 * 10^{-36} F$ and R to be unphysical (varyingly large and negative). $\tilde{\chi}^2$: 0.304 supports the value for our capacitance.

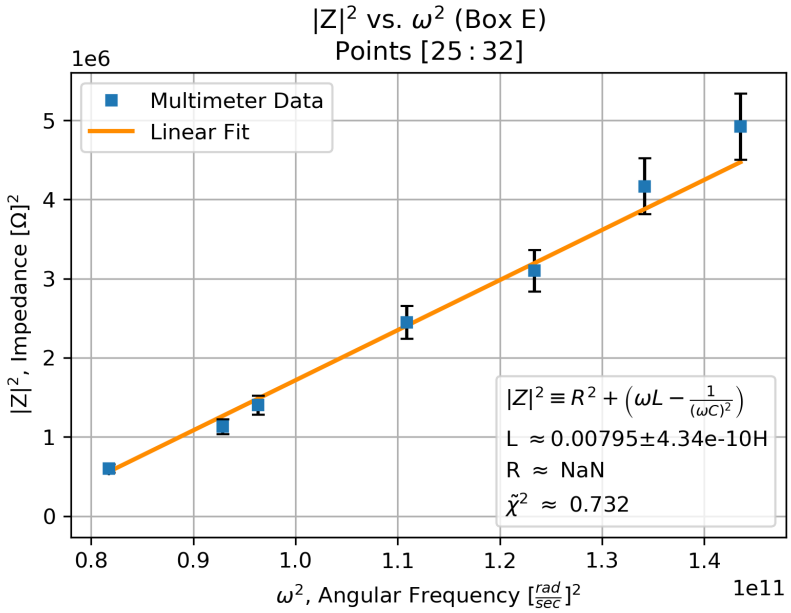

Figure 13. Mystery Box E's impedance^2 versus angular frequency^2. Here, we choose to truncate data, hoping to isolate the lower frequency data points in order to obtain an accurate value for the inductance (points [25:32] from supplied data table). Using the same RLC circuit assumption, we recover an inductance L $\approx 0.00795 \pm 4.34 * 10^{-10} H$. Again, we were unable to recover a physically meaningful value for the resistance (intercept), suggesting that there may be no obvious resistive component incorporated into mystery Box E. We back the legitimacy of our values with a reduced chi-square statistic $\tilde{\chi}^2$: 0.732.

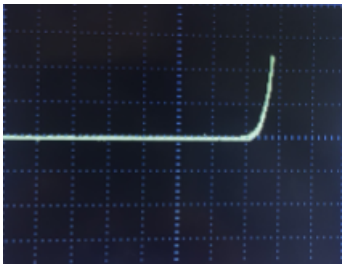

Figure 14. Box J's, an ordinary silicon diode with p-n type junction, qualitative, oscilloscope IV curve reading.

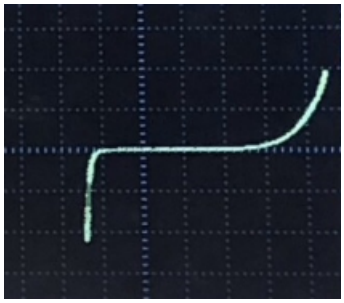

Figure 15. Box K's, a Zener diode with some negative breakdown voltage, IV curve with relevant characteristic seen qualitatively.